

Multi-scale modeling of the urban meteorology: integration of a new canopy model in the WRF model

Dasaraden Mauree^{a,b,*}, Nadège Blond^a, Alain Clappier^a

^aUniversité de Strasbourg, CNRS, Laboratoire Image Ville Environnement (LIVE), UMR7362, Strasbourg, France

^bSolar Energy and Building Physics Laboratory, Ecole Polytechnique Fédérale de Lausanne, Lausanne, Switzerland

Abstract

Urban parametrizations have been recently proposed and integrated in mesoscale meteorological models for a better reproduction of urban heat islands and to compute building energy consumption. The objective of the present study is to evaluate the value of the use of a module able to produce highly resolved vertical profiles of these variables. For this purpose, the Canopy Interface Model (CIM) was integrated as an additional urban physics option in the Weather Research and Forecasting model. The coupling method is here detailed and its evaluation is done using a reference run based on a fine resolution WRF simulation. In order to keep both the CIM and the mesoscale model coherent, an additional term is added to the calculation of the CIM. Finally, the BUBBLE dataset is used to validate the simulation of the profiles from CIM. It is demonstrated that the proposed coupling improves the simulations of the variables in an urban grid and that the WRF+CIM+BEP-BEM system can provide highly resolved vertical profiles while at the same time improving significantly computational time. The data from these preliminary results are very promising as it provides the foundation for the CIM to act as an interface between mesoscale and microscale models.

Keywords: Atmospheric boundary layer, Multiscale meteorological modeling, Turbulence parametrization, Urban canopy parametrizations, Urban meteorology

1. Introduction

Meteorological mesoscale models were initially dedicated to weather forecasting without the need to detail interactions between urban areas and the atmosphere (Salamanca et al, 2011; Ching, 2013). In the last few years, urban parametrizations have been integrated in these mesoscale models to also simulate urban heat islands (UHI) (Masson, 2000; Kusaka et al, 2001; Martilli et al, 2002; Kanda et al, 2005; Liu et al, 2006; Kusaka and Kimura, 2004; Sarkar and De Ridder, 2011), building energy consumption (Krpo et al, 2010) and air pollution at the urban scale (Salamanca et al, 2011). Different schemes have been developed in recent years with the underlying purpose of developing systems that could help urban planners make decisions and propose sustainable urban planning scenarios to decrease UHIs, building energy demand, or urban air pollution. Baklanov et al (2009) gave a guideline for the level of complexity that is needed for urban canopy parametrizations based on the “fitness for purpose”. For air quality, urban climatology, strategies to mitigate heat islands and urban planning, it is necessary to have more detailed and precise meteorological profiles and fluxes.

*Corresponding author

Email address: dasaraden.mauree@gmail.com (Dasaraden Mauree)
Preprint submitted to Elsevier

25 It is now well known that the urban climate depends on a series of processes taking place
26 at different spatial (from global to local) and temporal scales (Oke, 1982), and that building
27 energy demand and urban climate are closely related and interdependent (Ashie et al, 1999;
28 Kikegawa et al, 2003; Salamanca et al, 2011). However using mesoscale meteorological models,
29 with a high resolution, to cover a whole urban area and resolving at the same time local building
30 effects and urban heat islands is still not feasible with actual computer performances (Martilli,
31 2007). Moreover the use of available microscale models (such as Envimet (Bruse and Fleer, 1998),
32 CitySim (Robinson, 2012) or EnergyPlus (Crawley et al, 2008)) on more than a neighborhood
33 (few streets) is also not feasible. Thus multi-scale modeling is proposed as a solution.

34 Garuma (2017) has recently proposed a detailed review of urban surface parameterizations.
35 Previous developed models, such as those proposed by Masson (2000) or Kusaka and Kimura
36 (2004), have been integrated in mesoscale models. However since they are single-layered models
37 they do not calculate high resolution vertical profiles in the urban canopy. Using the same method
38 as Martilli et al (2002); Kondo et al (2005), who proposed a multi-layer model, Muller (2007)
39 designed experiments to show that a canopy module can be used for an enhanced coupling
40 with mesoscale models while at the same time reducing the computational cost. However in
41 their work, the canopy model developed by Muller (2007) was not totally independent of the
42 mesoscale model and hence cannot be easily introduced in another model. Furthermore, the
43 canopy model resolves flow in only one direction and hence is neglecting the horizontal advection
44 that is considered in a mesoscale model. Inconsistencies will thus arise between computations
45 done with a multi-layer microscale model such as BEP-BEM and a mesoscale model. One way
46 to ensure coherence in regional climate models (RCM), is to use nudging techniques to reduce
47 errors between the driving field and the simulated field (Pohl and Crtat, 2014; Omrani et al.,
48 2015).

49 The Canopy Interface Model (CIM) that was recently developed and tested in an offline
50 mode (Mauree, 2014; Mauree et al., 2015, 2017a) is here introduced in the Weather Research and
51 Forecasting (WRF) community research model v3.5 (Skamarock et al, 2005, 2008). The objective
52 is to build a multi-scale urban meteorological system that is able to produce highly resolved
53 vertical profiles of meteorological variables in low-resolution mesoscale meteorological models.
54 These profiles will then be used to improve the computation of surface fluxes of momentum,
55 heat, turbulent kinetic energy and humidity inside the mesoscale model and to allow at the same
56 time for the coupling of a mesoscale model with a microscale model. Such a coupling between
57 the CIM and CitySim, a micro-scale model to evaluate energy fluxes at the neighbourhood scale
58 has been proposed recently (Mauree et al., 2017b,c).

59 The objective of the present article is to detail the steps followed to set up and evaluate the
60 coupling. Indeed, a new method is proposed to ensure consistency between the models and to
61 take advantage of both models in the coupling system. When used with a low resolution, the
62 mesoscale model cannot reproduce correctly the vertical meteorological profiles and surface fluxes
63 in the canopy, but it still simulates the horizontal fluxes that are not considered in the CIM.
64 However the CIM is able to reproduce the vertical transport with enhanced precision. Similar
65 to nudging terms used in RCM, a correction of the CIM computations is thus proposed to add
66 horizontal fluxes effects in an effective way. Finally, the coupled system is ran over the City of
67 Basel and the results from the simulations are compared with observations.

68 In Sect. 2 a brief description of the governing equations in WRF is given and in Sect. 3 it will
69 be explained how the CIM has been integrated into WRF in order to keep in coherence both the
70 mesoscale model and the CIM. In Sect. 4 a description of the experiments conducted with WRF
71 is presented. In Sect. 5 the results from a series of sensitivity tests are presented to evaluate
72 the value of the use of the CIM and the proposed coupling. The last section is devoted to the
73 discussions and the conclusions of this study.

2. Weather Research and Forecasting model

The Advanced Research WRF (ARW)(Skamarock et al, 2005, 2008), version 3.5, developed by the National Center for Atmospheric Research (NCAR) for research purpose, is used in the present study and will be referred to hereafter as WRF. A broad variety of physics and dynamics options have been proposed by the scientific community. Only a brief description of the conservation equations and the physics options that are used to simulate the surface layer is given here. The objective of this section is mainly to help understand the coupling of the CIM with WRF, which will be fully described in Sect. 3.

2.1. Governing equations and turbulent closure

Following Ooyama (1990), variables with conservation properties (mass for example) are written with equations in their flux form and using a terrain-following mass vertical coordinate. We here present briefly these equations to prepare the presentation of the coupling with the CIM.

Momentum and Heat

The following equation represents the conservation of momentum or heat.

$$\partial_t N + (\nabla \cdot \vec{F}_N)_\eta = F_N^s, \quad (1)$$

where N is the momentum for the x -, y - or z -directions or the heat and F_N^s is the source or sink terms from the surface. The second term on the left hand side of the equation is a flux divergence term which represents the advection, the pressure-gradient and the diffusion terms. The latter is a function of the diffusion coefficients, $K_{h,v}$ which is described later. The $\nabla \cdot \vec{F}_N$ term depends the eta (η) levels and the latter can be computed using:

$$\eta = \frac{(p_h - p_{ht})}{\alpha}, \quad (2)$$

where p_h is the hydrostatic pressure at this height and p_{ht} is the pressure at the top boundary. α is the mass per unit area within the column in the domain and is calculated as $\alpha = p_{hs} - p_{ht}$ where p_{hs} is the pressure at the surface.

1.5 order turbulence closure

WRF provides several closure formulations for the calculation of the turbulent diffusion coefficients. A 1.5 order turbulence closure, using the turbulent kinetic energy (denoted hereafter as e , ($m^2 s^{-2}$)) is chosen here. With this closure the turbulent diffusion coefficient can be computed using:

$$K_{h,v} = C_k l_{h,v} \sqrt{E}, \quad (3)$$

where the subscript h, v represent horizontal and vertical directions respectively, C_k is a constant, $l_{h,v}$ is a parametrized mixing length, proportional to the height and E is αe .

Turbulent Kinetic Energy

The e can be calculated using the following prognostic equation:

$$\partial_t(E) + (\nabla \cdot \vec{F}_E)_\eta = \alpha(P + G - \varepsilon), \quad (4)$$

where P and G represent the mechanical and buoyancy turbulence production terms respectively and ε is the dissipation term.

More details on the chosen formulations can be found in Skamarock et al (2008).

111 *2.2. Focus on specific physics schemes*

112 WRF provides a large variety of physics schemes to represent different processes taking place
113 in the atmosphere. For the purpose of this study, the focus is mainly on specific schemes that
114 relate to future uses of the CIM.

115

116 **Surface layer scheme**

117 The surface layer schemes, proposed in WRF, calculate the friction velocities and exchange co-
118 efficients that enable the computation of surface heat and moisture fluxes by the land-surface
119 models and surface stress in the Planetary Boundary Layer (PBL). The Monin-Obukhov Simi-
120 larity Theory (Monin and Obukhov, 1954) option was chosen for this study.

121

122 **Land-Surface Model**

123 The Land-Surface Model (LSM) is a 1-D column model computing surface fluxes over land and
124 sea-ice grid point starting from land-surface properties and outputs of the surface layer scheme
125 and the radiation scheme. These fluxes give a lower boundary condition for the vertical transport
126 done in the PBL schemes. The Noah LSM (Chen and Dudhia, 2001) was selected.

127 Multiple urban physics options are available in WRF (UCM, BEP, BEP-BEM). We have
128 chosen to use the BEP-BEM parameterization (Salamanca et al, 2010) to simulate the buildings
129 effects on the long wave and short wave radiation (shadow effects and multi-reflexion) and the
130 surface fluxes of momentum and heat.

131 The Building Effect Parametrization (BEP) module is based on Martilli et al (2002) who
132 proposed a multi-layer model. Obstacle effects are estimated in several layers of the mesoscale
133 model. It takes into account the 3-D geometry of urban surfaces as well as the ability of buildings
134 to diffuse sources and sinks of heat and momentum vertically through the whole urban canopy
135 layer. The Building Energy Model (BEM), developed by Krpo et al (2010), computes the build-
136 ing energy balance (and the associated building demand) to keep a comfortable temperature
137 inside buildings. This energy balance takes into account the effect of anthropogenic heating and
138 heat diffusion through surfaces, radiation exchange through windows. The surface fluxes are
139 computed at each level of the urban grid and aggregated in BEP and are used as input in the
140 surface layer scheme.

141

142 **Planetary Boundary Layer**

143 The PBL scheme calculates flux profiles so as to compute the temperature, moisture and vertical
144 momentum profiles for the atmosphere. One important aspect of these types of schemes is that
145 they are one dimensional and assume that there is a clear separation between resolved and sub-
146 grid eddies (Skamarock et al, 2008). For the purpose of this study, the Bougeault and Lacarrère
147 turbulence closure scheme (Bougeault and Lacarrère, 1989) will be used to compute $l_{h,v}$, needed
148 for the calculation of the diffusion coefficient in the WRF model.

149 **3. Canopy Interface Model integration in WRF**

150 A 1-D Canopy Interface Model (CIM) was developed by Mauree et al. (2017a) in order to
151 improve low-resolution mesoscale meteorological models or to be used as an interface between
152 low-resolution meteorological mesoscale model and microscale models. After a brief description
153 of the CIM, it is explained in the present section how the CIM was introduced in WRF. CIM can
154 be typically forced at the top of the column and the variables are then calculated at the centre
155 of each cell along the vertical axis.

156 *3.1. Canopy Interface Model*

157 The CIM solves 1-D transport equations, i.e. only the terms in the z -direction are kept from
158 Eq. 1.

$$\frac{\partial u}{\partial t} = \frac{\partial}{\partial z} \left(\mu_t \frac{\partial u}{\partial z} \right) + f_u^s \quad (5)$$

$$\frac{\partial \theta}{\partial t} = \frac{\partial}{\partial z} \left(\kappa_t \frac{\partial \theta}{\partial z} \right) + f_\theta^s, \quad (6)$$

159 where u is the mean wind speed in the x - or y - directions (ms^{-1}), θ is the mean potential
160 temperature (K), f_u^s and f_θ^s are the momentum and heat surface fluxes and μ_t and κ_t are the
161 turbulent diffusion coefficients. κ_t is μ_t divided by the Prandtl number (0.95).

162 The CIM solves these equations using a 1.5 order turbulence closure based on the e . The
163 diffusion coefficient can be calculated using:

$$\mu_t = C_k l \sqrt{e}, \quad (7)$$

164 where C_k is a coefficient calculated to be equal to $k^{\frac{4}{3}}$, from [Mauree et al. \(2017a\)](#), where k is
165 the von Kàrmàn constant (0.41), l is the mixing length (m) and e is calculated independently as
166 follows:

$$\frac{\partial e}{\partial t} = \frac{\partial}{\partial z} \left(\lambda_t \frac{\partial e}{\partial z} \right) + C_\varepsilon^* \frac{\sqrt{e}}{l} (e_\infty - e) + f_e^s, \quad (8)$$

167 where λ_t is here assumed to be equal to μ_t ([Muller, 2007](#)) and e_∞ is a stationary e value as
168 explained by [Mauree et al. \(2017a\)](#) and can be expressed as:

$$e_\infty = \frac{C_k}{C_\varepsilon^*} l^2 \left(\frac{\partial U}{\partial z} \right)^2 (1 - C_G \cdot Ri_f), \quad (9)$$

169 where U is the horizontal wind speed (ms^{-1}), C_ε^* is equal to 1 and C_G is a correction coefficient
170 for the buoyancy term.

171 As the scope of the current study is beyond the development of the CIM, further details
172 about its governing equations and the calculation of the fluxes used in the model can be found
173 in [Mauree et al. \(2017a\)](#).

174 *3.2. WRF-CIM coupling strategy*

175 The CIM computes highly resolved vertical profiles of various meteorological variables, but
176 it does not include horizontal fluxes like a mesoscale model such as WRF (see Eq. 1). In such
177 a context, it is possible to force the CIM with WRF in a one-way nesting but it will not be
178 valuable to correct the values calculated by WRF using the CIM values as it could have been
179 proposed in a traditional two-way nesting.

180 Thus two methodologies are tested : the first one is based on a coupling using fixed top
181 boundary conditions as done by [Muller \(2007\)](#) ; the second is a new proposition to add an ad-
182 ditional term in the CIM calculation in order to account for the processes described by the flux
183 divergence term in Eq. 1.

184

185 **Coupling by Fixing Top boundary condition (Method FT)**

186 The CIM can calculate vertical profiles using prescribed top boundary conditions and the ge-
187 ometry and surface temperature of the surface obstacles at each level of the grid (see Fig. 1).
188 In an offline mode, the boundary conditions may be fixed at the top with a constant value.
189 When coupled with a mesoscale model, this value is linearly interpolated from the mesoscale

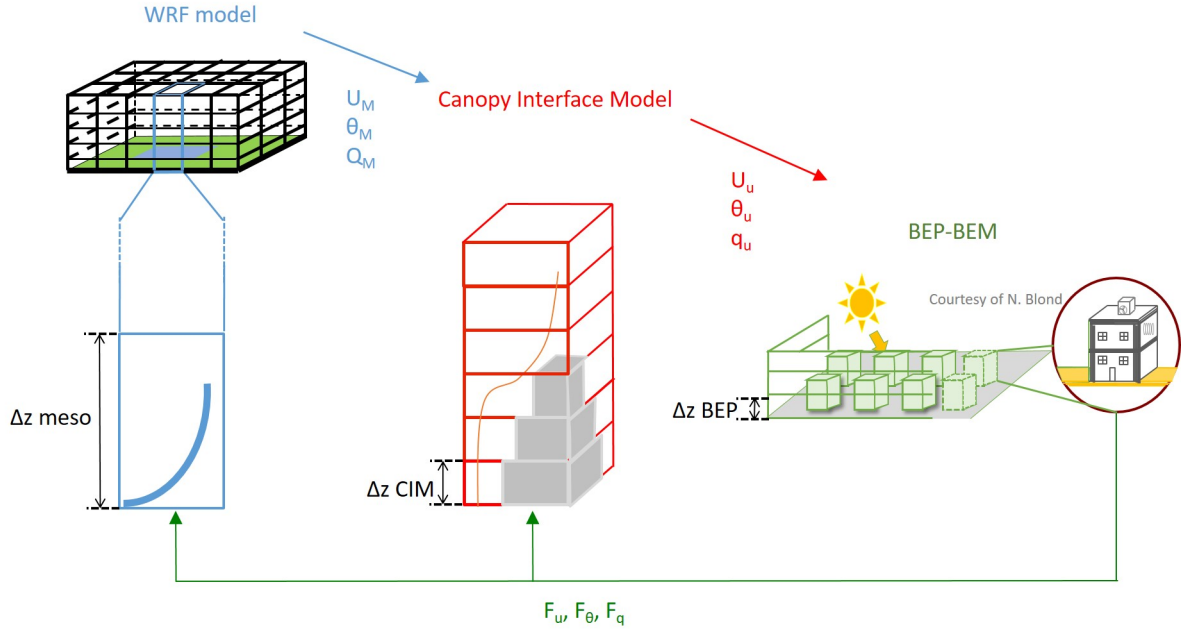


Figure 1: WRF scheme with the implementation of the CIM (arrows and variables in blue denotes items from WRF, in red from the CIM and in green from BEP-BEM)

190 model at each timestep (Martilli et al, 2002). At the initialization timestep, the mesoscale values
 191 are interpolated on each of the CIM vertical level and used to initialize the computation of the
 192 surface fluxes done by the BEP-BEM system (Krpo et al, 2010). At other timesteps, the CIM
 193 high-resolution vertical profiles (wind speed, temperature and humidity) are given to BEP-BEM
 194 which then proceeds to a potentially more detailed estimation of sources/sinks. The sources and
 195 sinks are then given back to the CIM to compute new vertical profiles, and to the mesoscale
 196 model (the surface fluxes are in this way aggregated at each of the mesoscale vertical levels and
 197 represent the F_N^s terms in the Eq. 1).

198 This coupling may be enough when the mixing boundary layer is well developed but could be
 199 limited in stable conditions when the exchanges between air layers are low. Indeed, in such cases
 200 the horizontal fluxes cannot be neglected as compared to the vertical fluxes and this method will
 201 not conserve the coherence between the two models from a flux standpoint.

202

203 Coupling by Fixing Fluxes (Method FF)

204

205 To keep the coherence between the models, we propose in this section a method, similar to a
 206 nudging technique, to take into account the horizontal transport in the CIM as well as a new
 207 forcing term at the top of the CIM using fluxes. To develop this, an analysis of the budget of the
 208 fluxes is done over the vertical column of the CIM and for the corresponding volume from the
 209 mesoscale model. Figure 2 gives a representation of the fluxes considered in both the CIM and
 210 the mesoscale model. The following hypotheses can be made to ensure the coherence between
 the models and a balance of the fluxes:

- 211 • The mean value of each variable calculated on the CIM column should be the same as the
 212 one computed by the mesoscale model (both models proposing an estimation of the same

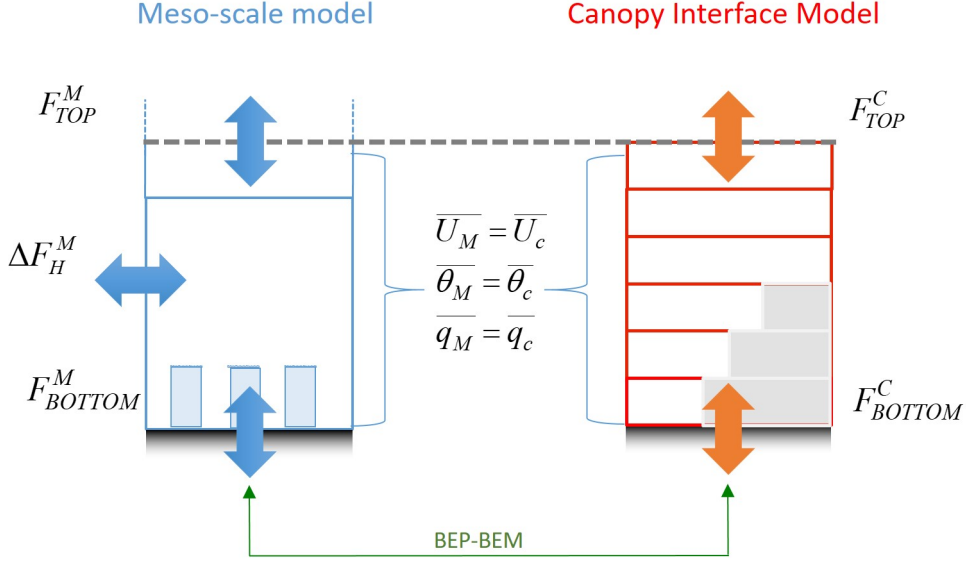


Figure 2: Representation of fluxes calculated on the vertical column in the CIM (right) before correction and in the corresponding volume in WRF (left). The average values from the meso-scale model and from the CIM should be equal in both models for the same volume. The grey dashed line represent the top most level of the CIM and can be higher than the first level of the meso-scale model.

213 real profiles);

- 214 • Bottom surface fluxes (i.e., all surface fluxes calculated to take into account the effects of ob-
- 215 stacles at each level of the column) are computed once for forcing both the mesoscale model
- 216 and the CIM. The values should hence be equal in both models ($F_{BOTTOM}^M = F_{BOTTOM}^C = F_{BOTTOM}$);
- 217 • In the mesoscale model, the fluxes are aggregated in BEP and used in the constant-flux
- 218 theory ($F_{BOTTOM}^M = F_{TOP}^M$);
- 219 • Far enough from the surface, the flux at the top of both columns should be equal as it
- 220 would be less influenced by surface effects ($F_{TOP}^M = F_{TOP}^C = F_{BOTTOM}$).

221 Based on the above statements, the CIM profiles may be corrected after each timestep using an
 222 estimation of the horizontal fluxes. The formulation is done to allow computation of these values
 223 that are not known *a priori* in order to ensure a coherence between the models. Equation 10
 224 points out the consequences of this condition on the CIM new profiles.

$$N_i^{Ct+1} = \begin{cases} N_i^{C*} + \Delta F_{Hi}, & \text{for } i < n \\ N_n^{C*} + \Delta F_{Hi} - \Delta t F_{TOP}, & \text{for } i = n, \end{cases} \quad (10)$$

225 where N is one of the variables calculated by the CIM (wind speed, potential temperature or
 226 humidity), t is the timestep considered, i is an index corresponding to the centre of a grid cell
 227 in the CIM and n is the number of levels in the urban grid. N_i^{Ct+1} is the updated vertical value
 228 of the CIM considering that N_i^{C*} is a first computation of the CIM without considering the
 229 horizontal fluxes and ΔF_{Hi} the horizontal terms to be added. A different equation is proposed

230 for the top most level of the CIM with N_n^{C*} being the value computed by the CIM without
 231 considering the top flux, Δt is the time step and F_{TOP} the flux at the top as explained before
 232 (and is oriented in the z -direction). This top flux may be used, instead of forcing the boundary
 233 conditions at the top of the CIM with values of wind, temperature or humidity.

234 To ensure coherence between the models using these formulations, we can write that the
 235 mean value of the variables calculated by the CIM have to be equal to the mesoscale value:

$$\overline{N_i^{Mt+1}} = \overline{N_i^{Ct+1}} = \overline{N_i^{C*}} + \overline{\Delta F_{Hi}} - \frac{\Delta t F_{TOP}}{n}, \quad (11)$$

236 where $\overline{N_i^{Mt+1}}$ is the mean mesoscale value interpolated from the mesoscale model over the n
 237 levels present in the CIM column similar to what is performed by Martilli et al (2002). As a
 238 first approximation, the horizontal terms can be assumed constant over the CIM column (equal
 239 to their mean) and these are computed using Eq. 11 as:

$$\Delta F_{Hi} = \overline{\Delta F_{Hi}} = \overline{N_i^{Mt+1}} - \overline{N_i^{C*}} + \frac{\Delta t F_{TOP}}{n}. \quad (12)$$

240 This then leads to Eq. 13, which gives the new formulations used in the CIM.

$$N_i^{Ct+1} = \begin{cases} N_i^{C*} + \frac{\overline{N_i^{Mt+1}} - \overline{N_i^{C*}} + \frac{\Delta t F_{TOP}}{n}}{\Delta t}, & \text{for } i < n \\ N_n^{C*} + \frac{\overline{N_i^{Mt+1}} - \overline{N_i^{C*}} + \frac{\Delta t F_{TOP}}{n}}{\Delta t} - \Delta t F_{TOP}, & \text{for } i = n \end{cases} \quad (13)$$

241 In this way, the results from the CIM and the mesoscale models should be consistent and the
 242 departures between the driving and driven fields should be reduced.

243 4. Experiments with WRF-CIM

244 4.1. Evaluation of the coupling methods

245 A series of simulation are designed to assess the value of the use of the CIM in WRF and
 246 particularly to see how the CIM can improve the meteorological vertical profiles when using a
 247 coarse vertical resolution and its impact on the computational time.

248 A domain of 20*20 cells was designed and each cell has a horizontal resolution of 45 km*45
 249 km. The domain was centered at latitude 48.404 °N and longitude 2.248 °E, situated near
 250 the “Ile-de-France” region in France, such that the topography did not interfere with the tests
 251 that have been conducted. The influence of the topography will be studied in future paper. A
 252 homogeneous urban area of 9 cells at the centre of the domain has been designed with building
 253 heights of 25m and the land use for the rest of the domain was taken from the MODIS database.
 254 The aim of these simulations is to demonstrate the validity of the proposed methods.

255 Several simulations were performed with WRF, all using the urban parametrization BEP-
 256 BEM (see Table A.4), over a winter period of 30 days from the 27th of January 2010 at 0000
 257 LT to the 26th of February 2010 at 0000 LT (with the first three days of initialization not being
 258 discussed here).

259
 260 WRF is run for all the simulations using the BEP-BEM parameterization for the urban
 261 effects. The vertical resolution, the use of CIM and the choice of the method are changed for the
 262 different scenarios:

263 **Reference Simulation (Ref.)** : WRF is run with a fine vertical resolution of 5 m (corre-
 264 sponding to the vertical resolution of the CIM) for the first 15 levels), without the CIM. This

Table 1: Set of experiments run for theoretical case.

Simulations	Designation	Vertical resolution	Method
BEP-BEM	Ref.	Fine res. - 5m (15 levels)	
BEP-BEM	C1	Coarse res. - 94m (1 level)	
CIM+BEP-BEM	C3	Coarse res. - 94m (1 level)	FF
CIM+BEP-BEM	C5	Coarse res. - 94m (1 level)	FT

FF (fixed flux) and FT (fixed top) represent the two coupling methods.

265 is considered to be the reference simulation. The simulation integrates all processes needed to
 266 calculate highly resolved vertical profiles used by BEP-BEM for computing the urban effects.

267 **Simulation C1** : WRF is run with a coarse vertical resolution of 94 m, for the first level, without
 268 the CIM. This simulation, compared to the reference one, will show the impact of the vertical
 269 resolution on the surface representation and on the calculation of the meteorological variables in
 270 the WRF model.

271 **Simulation C3** : WRF is run with a coarse vertical resolution with the CIM coupled using
 272 Method FF. BEP-BEM runs with the CIM profiles. This test is performed to see how the pro-
 273 files that are calculated by the CIM, when it is integrated in the WRF model, correspond to
 274 those from the reference simulation and how this will in turn influence the mesoscale processes
 275 in a low resolution simulation.

276 **Simulation C5** : WRF is run with a coarse vertical resolution with the CIM coupled using
 277 Method FT. This test is performed to compare with the FF method in a low resolution simula-
 278 tion.

279 It should be highlighted here that we consider the Ref. simulation as a controlled experiment
 280 which we can use to assess the proposed methods (FF and FT) and it can be relied on as the
 281 scheme that integrates most of the physical processes. Additionally another set of simulation
 282 is performed to evaluate the impact of using a high resolution in WRF and this is included in
 283 [Appendix A](#).

284 4.2. Validation of CIM integration in WRF

285 To validate the integration of CIM in WRF, a set of simulation was run over Basel for a
 286 period of 14 days from the 1 January 2002 at 0000 LT to the 15th of January 2002 at 0000
 287 LT. Two scenarios were performed one with WRF+BEP-BEM and one with WRF+CIM+BEP-
 288 BEM. The four domains centred over the City of Basel with the different domains having a
 289 horizontal resolution of 45km, 15km, 3km and 1km respectively. The domain was designed
 290 using the WRFDomain wizard, allowing an optimal number of eta levels in the 1km and also for
 291 describing the bounding boxes. The GRIB data was downloaded from the UCAR dataset ([NCEP
 292 et al., 2000](#)). CSV files with the values (from CIM and as calculated by WRF) of the horizontal
 293 wind speed in both directions and the temperature for each vertical level were obtained from the
 294 simulation for comparison with measured data from the BUBBLE experiment ([Rotach et al.,
 295 2005](#)). All the data from BUBBLE and the simulation were averaged over one hour.

296 5. Results

297 This section aims at evaluating the coupling between the CIM and WRF and to justify the
 298 strategy that has been developed. As previously mentioned, the simulations presented here were
 299 performed for a period of 30 days (with the first three days of initialization not being discussed

300 here) in January 2010. We only show results for the horizontal wind speed and the temperature
301 for this corresponding period.

302 *5.1. Global comparisons on specific vertical levels*

303 We present here the comparisons over 27 days of simulation, in January, and a series of sta-
304 tistical tests in order to show the general trends when the CIM is integrated in WRF in winter.
305 Table 2 summarizes the comparisons in terms of mean biases, correlations and the root mean
306 square errors (R.M.S.E) computed on hourly values of the simulated temperatures and wind
307 speeds. Figure 3 presents a time-evolution of the different simulations at 5 m and 50 m. The
308 results from each scenario as compared to the reference case are discussed below.

310 *5.1.1. Effect of the WRF vertical resolution - (Ref./C1)*

311 We focus here on the differences observed between the fine and coarse resolution WRF sim-
312 ulations, without the CIM, as increasing the vertical resolution can have a remarkable effect on
313 the temperature and the wind speed. It can indeed be seen from Table 2 that, on average, the
314 coarse WRF configuration (C1) generally tends to over-estimate the potential temperatures and
315 to significantly under-estimate the wind speed as compared to the reference simulation.

316 Figure 3a shows that the differences in temperature may be more than 2 K for some hours.
317 The horizontal wind speed computed at 50 m is weaker in the coarse resolution simulation than
318 in the fine resolution simulation and these differences may reach 4 m s^{-1} . These first results
319 hence justify the development of the CIM model and its coupling with WRF since the changes
320 in the vertical resolution have a significant influence on the accuracy of models to calculate tem-
321 perature and wind profiles.

323 *5.1.2. Effect of the FF coupling with the CIM at low resolution - (Ref./C3)*

324 When using a coarse resolution in the model, the integration of the CIM in WRF drastically
325 the average difference, for the wind speed, decreased from -1.9 m s^{-1} to -0.9 m s^{-1} at 50 m
326 and reduces the over-estimations of the temperature from 0.3 K to 0.1 K (see Table 2). It can
327 however also be noted that in some cases the temperature is still under-estimated by about 1
328 K. If we focus on the high vertical resolution profiles that the CIM produces, it can be seen
329 that for the wind speed the bias is even decreased to -0.6 m s^{-1} at 50 m while also respecting
330 their variability (high correlation coefficient). Although the wind speed from the CIM at 50 m
331 is generally in agreement with the fine resolution simulation, there are a few hours where the
332 difference can be up to 1 m s^{-1} (see Fig. 3b). However, the CIM under-estimates the wind speed
333 at 5 m (bias of -1.2 m s^{-1}) and the variability of these values is not as well represented, at the
334 surface, as compared to the values obtained at 50 m. But as shown in Fig. 3d the amplitude is
335 also less important at 5 m than at 50 m. It is worthy to note that there are significant periods
336 when the CIM has a very good correspondence with the fine resolution simulation.

338 *5.1.3. Effect of the FT coupling - (Ref./C5)*

339 In order to show the importance of the coupling methodologies proposed, Table 2 also presents
340 the results of a comparison between the WRF fine resolution simulations and the WRF-CIM
341 simulations without taking into account the horizontal fluxes (C5). It can be noted that when
342 the horizontal fluxes are removed the bias and the R.M.S.E increase for both the temperature
343 and the wind speed as compared to the simulation where the fluxes were present (except for the

Table 2: Statistical comparison between the Reference Simulation (Ref.) and simulations C1, C3 and C5.

Simulations	Method				
	FF	FT	Mean bias	R.M.S.E	R
<i>For Potential Temperature (K)</i>					
WRF+BEP-BEM					
Meso outputs at 50 m					
Coarse Res. C1			0.3	0.9	0.98
WRF+CIM+BEP-BEM					
Meso outputs at 50 m					
Coarse Res. C3	x		0.1	0.9	0.98
Coarse Res. C5		x	0.0	0.9	0.98
CIM outputs at 50 m					
Coarse Res. C3	x		0.0	1.0	0.98
Coarse Res. C5		x	0.1	0.9	0.98
CIM outputs at 5 m					
Coarse Res. C3	x		0.3	0.9	0.98
Coarse Res. C5		x	0.7	1.2	0.98
<i>For Wind ($m s^{-1}$)</i>					
WRF+BEP-BEM					
Meso outputs at 50 m					
Coarse Res. C1			-1.9	2.0	0.98
WRF+CIM+BEP-BEM					
Meso outputs at 50 m					
Coarse Res. C3	x		-0.9	1.0	0.98
Coarse Res. C5		x	-0.2	0.9	0.97
CIM outputs at 50 m					
Coarse Res. C3	x		-0.6	0.9	0.97
Coarse Res. C5		x	-0.2	0.7	0.98
CIM outputs at 5 m					
Coarse Res. C3	x		-1.2	1.5	0.59
Coarse Res. C5		x	-1.2	1.6	0.36

Comparisons are made for all the mesoscale outputs and for the CIM outputs for scenarios C3 and C5. FF (fixed flux) and FT (fixed top) represent the two coupling methods. Mean bias represents the deviation from the reference simulation, R.M.S.E is the root mean square error and R is the correlation. Meso outputs refers to outputs from the meso-scale model WRF, CIM outputs refers to outputs directly from CIM and 5m and 50m refers to the height at which the data is taken.

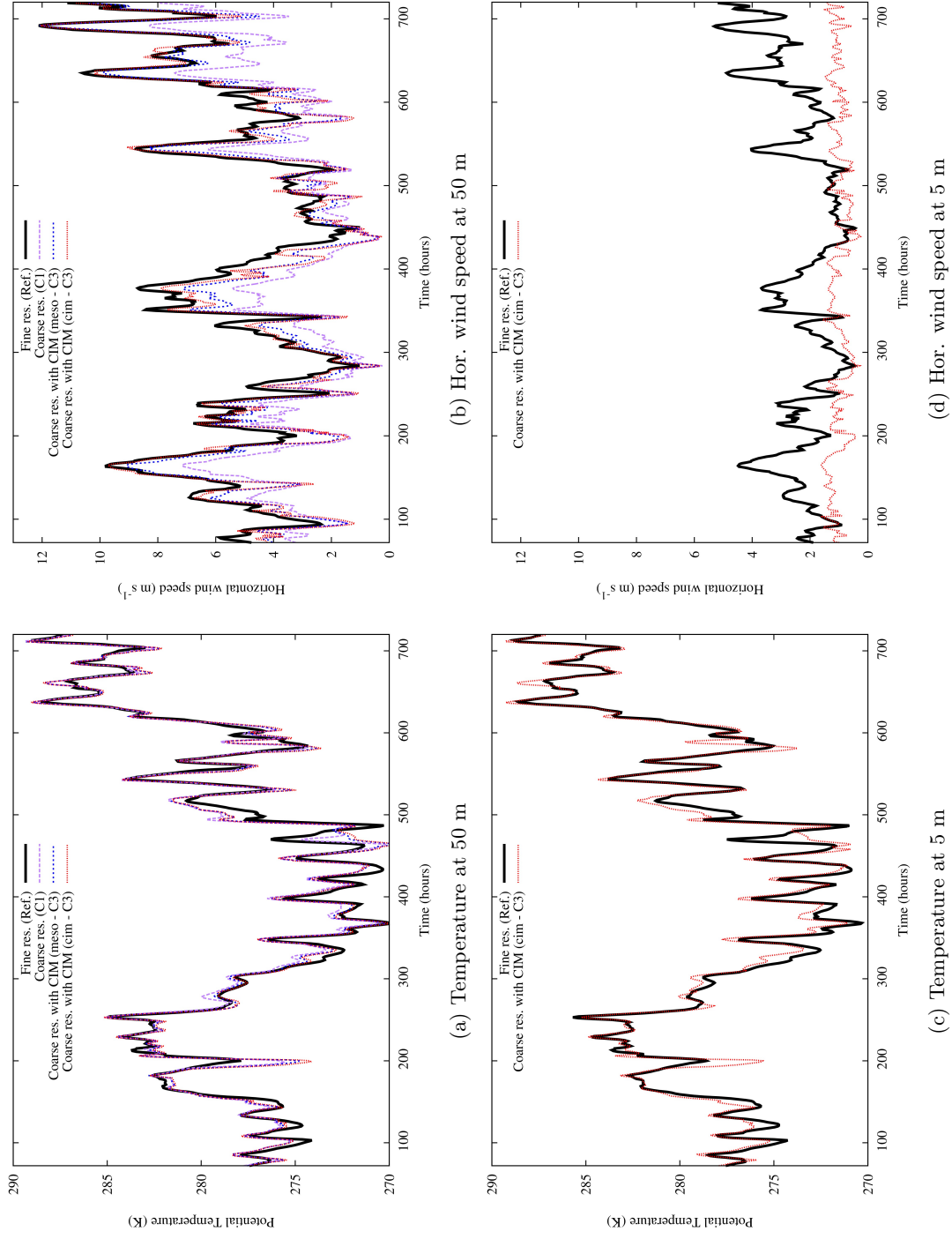


Figure 3: Comparison of the potential temperature (in K) (left) and wind speed (in m s⁻¹) (right) computed using WRF without and with the coupling of the CIM at 50 m (top) and at 5 m (bottom). Black lines refer to reference simulation (Ref.), purple refer to C1, blue lines refer to mesoscale values from C3 (meso - C3) and red lines refer to the CIM values from C3 (cim - C3). Horizontal axis represents the time, in hours, after the start of the simulation

344 wind speed at 50 m from the mesoscale model). The correlation coefficient for the wind speed
345 at 5 m is also drastically reduced.

346 Even though we know that in the CIM the vertical fluxes and diffusion processes are better
347 taken into account, we cannot conclude that the results are better in this context. The mesoscale
348 model contains a number of processes, such as the horizontal wind advection or pressure gradient,
349 which are not taken into account. It is thus important to take these processes into account in
350 the CIM in such a way that both calculations from the CIM and WRF remain coherent. This
351 thus justifies the use of the FF method.

352 5.1.4. Summer results

353 Simulations were also performed over a summer period of 1 month in July 2010. Since the
354 results from this period showed similar behaviour to the results for the winter case they will be
355 only briefly discussed here. The integration of the CIM in the WRF model improved the results
356 when comparing to the simulation without the CIM using a coarse resolution. A decrease in
357 the bias for both the temperature (from 0.5 K to 0.4 K) and the horizontal wind speed (from
358 -1.1 m s^{-1} to -0.3 m s^{-1}) were noted for the mesoscale data at 50 m. The correlations for the
359 temperature (0.99 to 1) were generally good as for the winter case. As for the profiles calculated
360 by the CIM, it is noteworthy to mention that when the horizontal fluxes were not present, there
361 was a significant increase in bias for the temperature at 5 m (from 0.1 K to 1.8 K) while for the
362 wind speed the results were not significantly very different for both cases.

363 5.2. Comparison on specific vertical profiles

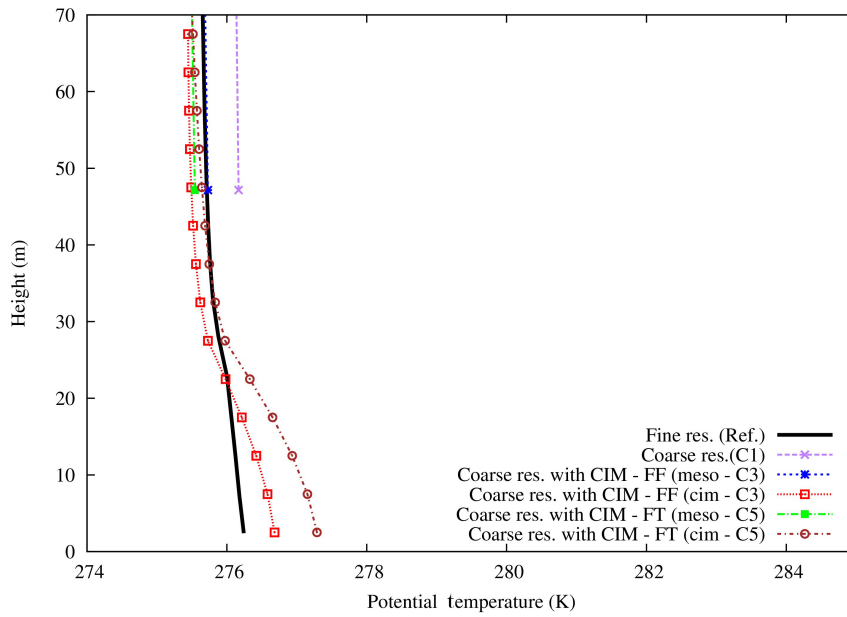
364 Selected vertical profiles for specific time steps are chosen to illustrate the effect of the cou-
365 pling methods in different atmospheric stability conditions. From the time-evolution profiles of
366 the mean wind speed and potential temperature (Fig. 3), we chose some specific periods to plot
367 vertical profiles for one grid cell (the centre of the urban area) for the different scenarios.

369 5.2.1. Comparison using a coarse vertical grid resolution in the mesoscale model

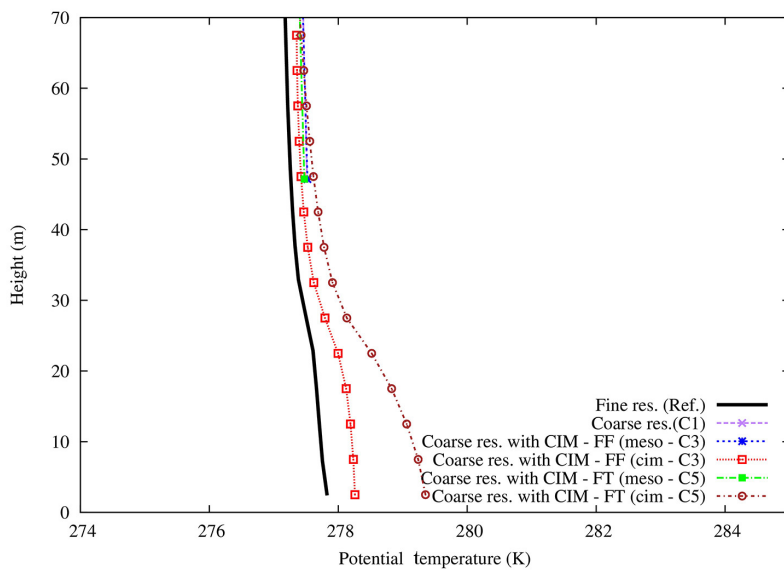
370 The differences between the profiles calculated by the CIM and by the mesoscale model
371 were studied on an hourly basis and were found to be minimal during the morning when the
372 development of the boundary layer was at a maximum. We thus chose two vertical profiles out
373 of this zone to show that the CIM can perform in near-neutral (stable) or unstable conditions.
374 Figures 4 and 5 show the comparisons of the vertical profiles obtained by the mesoscale model
375 when used at coarse resolution without or with the CIM (Ref., C1 and C3). In the same way
376 as the previous experiences with a high resolution, when the CIM is used, the effect of the FT
377 coupling method is also tested (C5).

378 At 0200 LT the potential temperature calculate by the meso-scale model (meso-C3) corre-
379 sponds to the one calculated by the fine resolution mesoscale simulation (Ref.). At 1700 LT,
380 there is a global difference of less than 0.5 K between the profile calculated (meso-C3) and the
381 fine resolution (Ref.). In both cases the profiles from CIM (cim-C3) are in very good agreement
382 with the Ref. profile. In the absence of horizontal fluxes, the temperature is over-estimated over
383 the whole column of the CIM and the difference is increased to more than 1.5 K in the first 10
384 metres. It is noteworthy to mention that the correction does not change the stability regime of
385 the atmosphere.

386 The horizontal wind speed in a near-neutral situation, for example at 0200 LT, (see Fig. 5a),
387 is significantly improved for the mesoscale model, when using a coarse resolution. It can be
388 highlighted here that at 50 m the wind speed is increased from 2 m s^{-1} to over 3 m s^{-1} . The
389 profiles which are calculated from the CIM are also in very good agreement with the reference

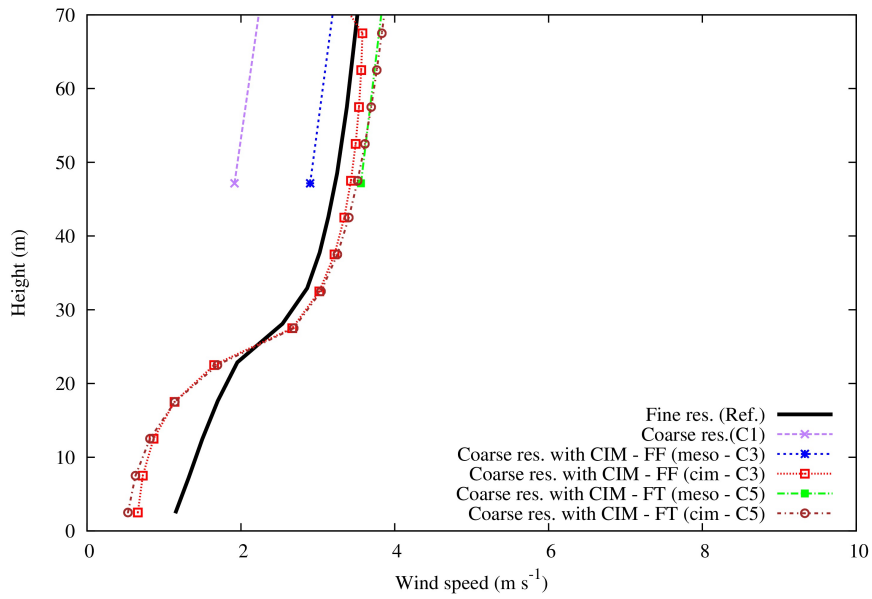


(a) At 0200 LT

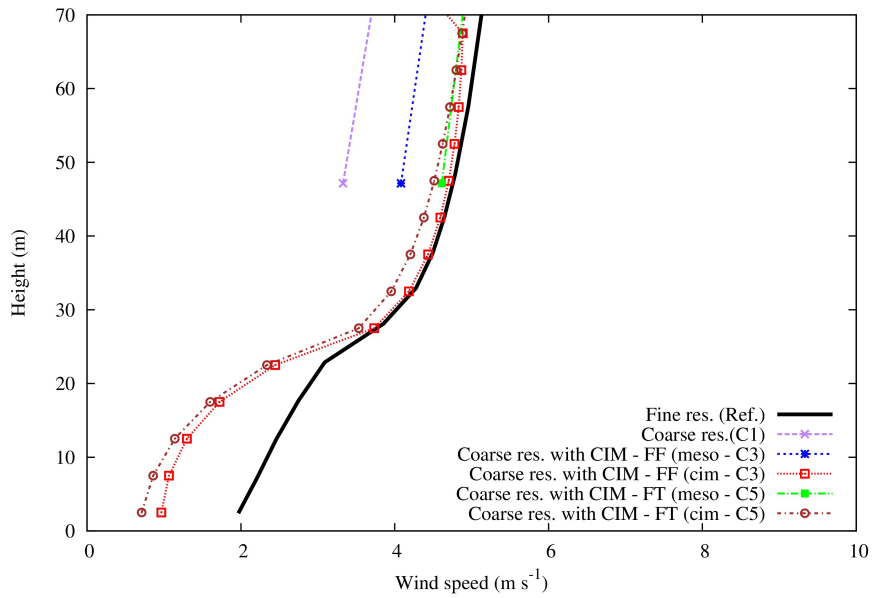


(b) At 1700 LT

Figure 4: Profile of the potential temperature (in K) using a fine resolution with WRF (Ref. - bold black curve), coarse resolution (C1 - purple curve), coarse resolution with the CIM (meso - C3 - blue curve ; cim - C3 - red curve) and coarse resolution with the CIM - with no horizontal fluxes (meso - C5 - green curve ; cim - C5 - brown curve)



(a) At 0200 LT



(b) At 1700 LT

Figure 5: Profile of the wind speed (in m s^{-1}) using a fine resolution with WRF (Ref. - bold black curve), coarse resolution (C1 - purple curve), coarse resolution with the CIM (meso - C3 - blue curve ; cim - C3 - red curve) and coarse resolution with the CIM - with no horizontal fluxes (meso - C5 - green curve ; cim - C5 - brown curve)

Table 3: Computational time (in minutes) needed to run the model for each of the simulations

Simulations	Computational Time
Ref.	63 minutes
C1	48 minutes
C3	49 minutes
C5	49 minutes

simulation. If the horizontal fluxes are removed, the wind speed above the canopy is slightly under-estimated in the CIM.

The results are more contrasted in an unstable condition, such as at 1700 LT (see Fig. 5b). The profiles calculated by the CIM with the horizontal fluxes are closer to the reference simulation (less than 0.5 m s^{-1} difference). However, if we look at the mesoscale profiles, we can observe that the profile calculated using the method without the horizontal fluxes is much closer to the reference solution. This can also be explained with the method that we have proposed for the calculation of the horizontal fluxes. This correction was proposed by using a mean value for the canopy as well as a mean value for the mesoscale model over the corresponding volume. In order to be in agreement with this statement, if one wants to calculate a coherent profile in the CIM, then there is a slight deterioration of the mesoscale value.

It should also be noted here that in the simulation without horizontal fluxes, the value is fixed at the top boundary conditions. We evaluated in this way two possibilities for fixing the boundary condition at the top. We determined, from these experiments, that the addition of the horizontal fluxes were more important as compared to fixing the top boundary conditions, in order to keep the coherence between both models.

5.3. Computational time

Finally an analysis of the computational time was made. Table 3 summarizes the CPU time used for several simulations.

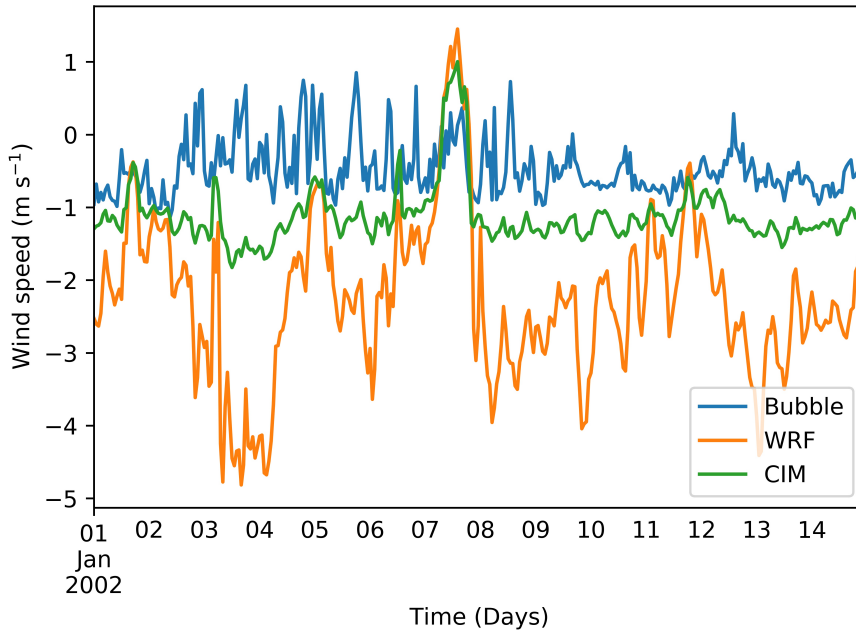
The data highlights the fact that when the vertical resolution of WRF is decreased, the computational time is significantly decreased (around 25% less). When the CIM is introduced, the computational time is not impacted even though there is an additional calculation which is now being performed by the system to produce high resolution profiles. This means that this coupled WRF-CIM system is able to produce an enhanced simulation without significantly increasing the computational time.

5.4. Validation over Basel using BUBBLE data

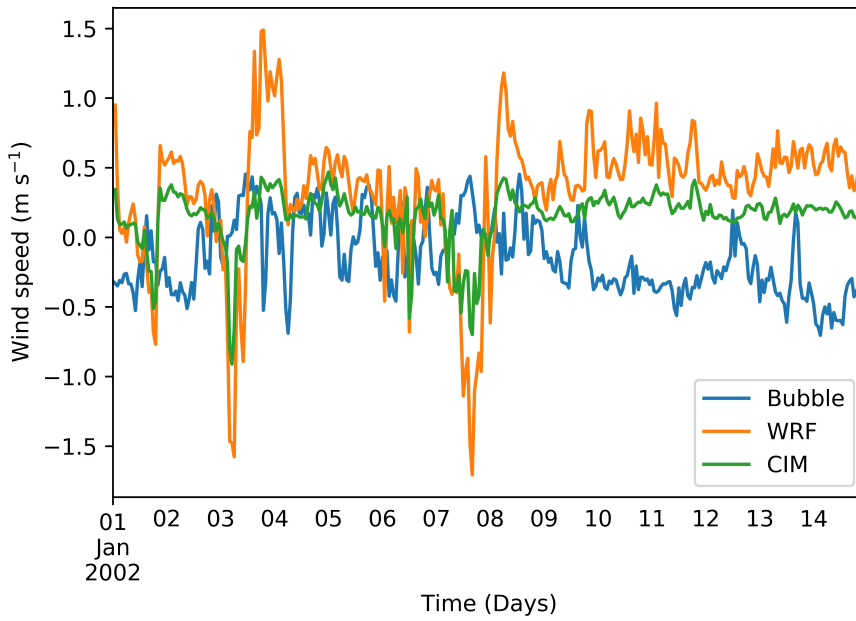
Two scenarios were run over Basel from the 01/01/2002 to the 14/01/2002. Wind speed and temperature data from the simulation were obtained from a grid cell centred around the coordinates 47.56N, 7.59E. This corresponds to the location of the tower installed during the BUBBLE experiment to which the simulated data are compared.

Figure 6 shows the wind speed for the x - and y -directions at a height of 3m from the BUBBLE data and from CIM while for the WRF data is the value for the first vertical level typically used for forcing BEP-BEM or any other UCMS in the WRF model. It can clearly be seen that the CIM data is much closer to the BUBBLE data as compared to the WRF data. The difference is more striking for the u -values. Nonetheless, it is evident that since the WRF data are used as boundary conditions for the CIM, there is a very good correlation between them.

When looking at the horizontal wind speed, the difference is even more visible (see Figure 7a). It can again be highlighted there the CIM data is much closer to the BUBBLE data as compared

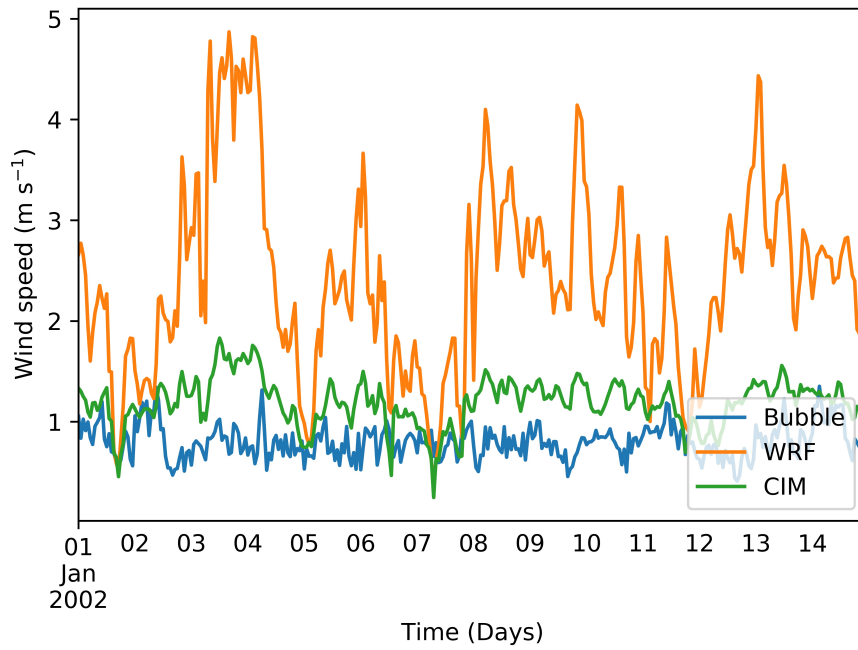


(a) Wind speed in the x -direction

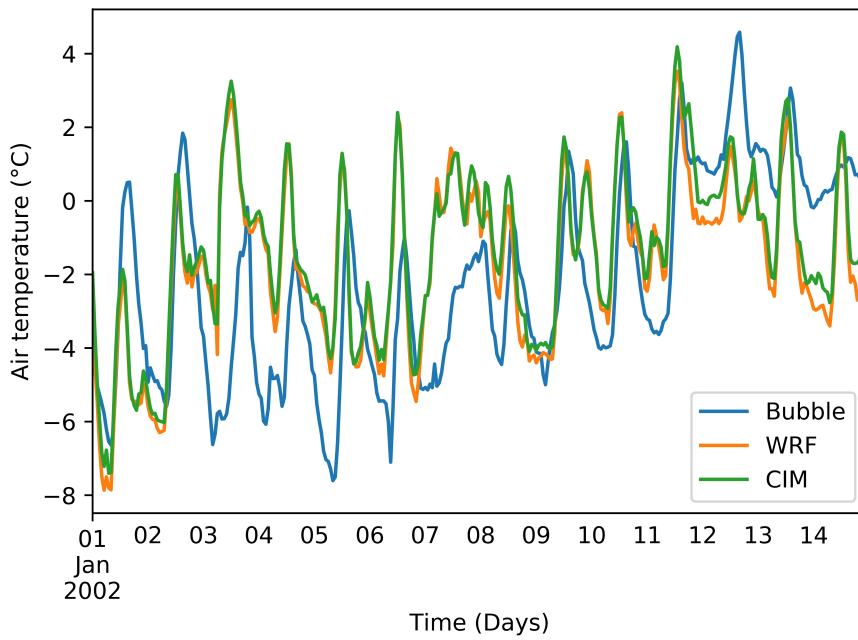


(b) Wind speed in the y -direction

Figure 6: Comparison of the wind speeds (in m s^{-1}) from the BUBBLE experiment (in blue), from WRF (in orange) and from CIM (in green) from the 01/01/2002 to 14/02/2002.



(a) Horizontal wind speed (in m s^{-1})



(b) Air temperature ($^{\circ}\text{C}$)

Figure 7: Comparison of the horizontal wind speed (in m s^{-1}) and the air temperature ($^{\circ}\text{C}$) from the BUBBLE experiment (in blue), from WRF (in orange) and from CIM (in green) from the 01/01/2002 to 14/02/2002.

428 to the standard WRF data. Figure 7b shows the air temperature as measured by BUBBLE and
429 calculated by WRF and CIM. Both WRF and CIM are able to reproduce the daily dynamics of
430 the air temperature but CIM falls short of improving significantly the results from WRF. There
431 are some periods for example on the 12/01 and on the 14/01 where the CIM results are closer to
432 the BUBBLE data but the difference between the simulated and measured data is still around
433 1°C. It can be pointed out that the discrepancy between the BUBBLE data and CIM could be
434 due to the over-estimation of the wind speed in some cases, particularly during midday.

435 6. Discussion and Conclusion

436 A Canopy Interface Model (CIM) was designed by Mauree et al. (2017a) in such a way that
437 it can act as an interface between mesoscale models and microscale models. In this study it
438 has been coupled with the Weather Research and Forecasting model (WRF). The aim of this
439 study was to evaluate the coupling done specially to improve surface representation in mesoscale
440 models and to demonstrate the ability of the system to provide valuable high-resolution vertical
441 profiles. The CIM is a standalone 1-D column model that can be forced only at the top using
442 values interpolated from the mesoscale model to calculate meteorological profiles independently
443 of the mesoscale model. However to keep the coherence between both the CIM and WRF, a new
444 method, similar to a nudging technique, was proposed so as to add an additional term, in the
445 CIM calculations, in order to take keep the consistency between the two models.

446 Using a theoretical setup and a series of sensitivity analysis and simulations, it was shown
447 that:

- 448 • When WRF was used with a coarse resolution, the coupling of the CIM and WRF was
449 closer to the reference simulations (we also verified that when WRF was used with the same
450 vertical resolution as the CIM, the simulations of both models were very similar and in
451 this way coherent). Compared to the highly resolved simulation, it was shown that WRF,
452 with a low resolution, tends to over-estimate the temperature and under-estimate the wind
453 speed. Coupled with the CIM, the new system showed better performances with smaller
454 R.M.S.E and biases. Usually the correlations were similar and very good.
- 455 • It was demonstrated that the correction brought to the CIM calculation to take into account
456 the horizontal fluxes was very important in order for both the mesoscale model and the
457 CIM to be in coherence.

458 Not all of the experiments that were conducted were presented here. A simulation was carried
459 out for a summer period and as the results showed similar behavior to the results presented in
460 this study, they were only briefly discussed. Tests were also conducted to evaluate the influence
461 of fixing a value at the top of the canopy or calculating a flux. There were no significant changes
462 between the two scenarios, but it is indeed more coherent to use a flux instead of fixing a value
463 at the top based on the method that we have proposed. This provides an enhanced degree of
464 freedom for the calculation in the CIM. We also analyzed the influence of having different vertical
465 resolutions for the first mesoscale grid cell. This did not show significant impact on the results
466 and therefore means that the CIM can be used independently of the height of the first level in
467 the mesoscale model. The assumption made, when describing the method “FF”, that the flux
468 at the top of the canopy has to be equal to the bottom flux, imposes that a constant-flux layer
469 needs to fully develop at the top of the column. It is thus essential to have a minimum number
470 of vertical levels in the CIM to achieve the best performance. It has previously been suggested
471 that the constant-flux layer developed at a height of twice the maximum height of the buildings
472 (?). This can thus be used as an indication of the number of levels required in CIM.

473 Furthermore, we validated the high-resolution vertical profiles by comparing the simulated
474 profiles from WRF and from CIM with data from the BUBBLE experiments. We demonstrated
475 that the horizontal wind speed was very close to the observed BUBBLE data and that there were
476 good agreement with the air temperature simulations. There are however some discrepancies in
477 the simulations which can further be investigated in the future. One example is that the wind
478 speed is still slightly over-estimated and this might be due to the parameterization of the drag-
479 force.

480 Further investigations are required to improve our comprehension of the processes taking
481 place at these different scales. The resolution of the turbulence closure in the CIM is different
482 from that of WRF: this would explain why close to the surface the CIM has a higher impact
483 than far enough from the surface. Moreover when a correction was brought to the CIM in
484 such a way that the CIM calculations were coherent with the mesoscale calculation, this meant
485 that the results in the mesoscale models were less affected in some cases, particularly in unstable
486 conditions. The WRF+CIM+BEP-BEM system also has to be tested on a more realistic domain
487 so that measured monitored data can be compared with the simulation results. An observational
488 campaign (MoTUS), measuring high resolution and high-frequency variables has been launched
489 on the EPFL campus, Switzerland to develop new parameterizations (Mauree et al., 2017d).

490 In conclusion of this study, we can say that the WRF+CIM+BEP-BEM system is able to
491 calculate coherent high resolution vertical profiles in the canopy and these profiles were in good
492 agreement with those calculated using WRF with a high vertical grid resolution. It was therefore
493 demonstrated that the CIM can be used in a low-vertical resolution mesoscale model to reduce
494 the computational cost and to improve results. In view of the above promising results, the foun-
495 dation for the use of the CIM as an interface to enhance surface representation and to couple
496 mesoscale models to microscale models is established.
497

498 7. Acknowledgements

499 The authors would like to thank ADEME, Region Alsace, REALISE, ZAEU for financial
500 supports. This work was partially done in the framework of the SCCER Future Energy Efficient
501 Buildings and Districts, FEEB&D (CTI.2014.0119), the ANR Trame Verte and the CCTV2
502 projects. The authors thank the High Performance Computing Centre of the Université de
503 Strasbourg (<http://hpc.unistra.fr>) where the system WRF-CIM was set-up and where the servers
504 were partially funded via the french Equipex project Equip@Meso. We would also like to thank
505 Alberto Martilli for the interesting discussions and Andreas Christen for the BUBBLE data.

506 8. References

- 507 Ashie Y, Thanh Ca V, Asaeda T (1999) Building canopy model for the analysis of urban climate.
508 J Wind Eng Ind Aerodyn 81:237-248. DOI 10.1016/S0167-6105(99)00020-3
- 509 Baklanov A, Grimmond CS., Mahura A, Athanassiadou M (2009) Meteorological and air quality
510 models for urban areas. Springer
- 511 Bougeault P, Lacarrère P (1989) Parameterization of orography-induced turbulence in a
512 mesobeta-scale model. Mon Weather Rev 117:1872-1890.
- 513 Bruse M, Fleer H (1998) Simulating surface-plant-air interactions inside urban environments
514 with a three dimensional numerical model. Environ Modell Softw 13:373-384. DOI 10.1016/
515 S1364-8152(98)00042-5

- 516 Chen F, Dudhia J (2001) Coupling an advanced land surface-hydrology model with the Penn
517 State-NCAR MM5 modeling system. Part I: Model implementation and sensitivity. *Mon*
518 *Weather Rev* 129:569-585.
- 519 A perspective on urban canopy layer modeling for weather, climate and air quality applications.
520 *Urban Climate* 3:1339. DOI <https://doi.org/10.1016/j.uclim.2013.02.001>.
- 521 Crawley DB, Hand JW, Kummert M, Griffith BT (2008) Contrasting the capabilities of building
522 energy performance simulation programs. *Build Environ* 43:661-673. DOI 10.1016/j.buildenv.
523 2006.10.027
- 524 Review of urban surface parameterizations for numerical climate models. *Urban Climate*. DOI
525 <https://doi.org/10.1016/j.uclim.2017.10.006>.
- 526 Kanda M, Kawai T, Kanega M, et al (2005) A simple energy balance model for regular building
527 arrays. *Boundary-Layer Meteorol* 116:423-443. DOI 10.1007/s10546-004-7956-x
- 528 Kikegawa Y, Genchi Y, Yoshikado H, Kondo H (2003) Development of a numerical simulation
529 system toward comprehensive assessments of urban warming countermeasures including their
530 impacts upon the urban buildings energy-demands. *Appl Energy* 76:449-466. DOI 10.1016/
531 S0306-2619(03)00009-6
- 532 Kondo H, Genchi Y, Kikegawa Y, et al (2005) Development of a multi-layer urban canopy model
533 for the analysis of energy consumption in a big city: Structure of the urban canopy model and
534 its basic performance. *Boundary-Layer Meteorol* 116:395-421. DOI 10.1007/s10546-005-0905-5
- 535 Krpo A, Salamanca F, Martilli A, Clappier A (2010) On the impact of anthropogenic heat fluxes
536 on the urban boundary layer: A two-dimensional numerical study. *Boundary-Layer Meteorol*
537 136:105-127. DOI 10.1007/s10546-010-9491-2
- 538 Kusaka H, Kondo H, Kikegawa Y, Kimura F (2001) A simple single-layer urban canopy model for
539 atmospheric models: comparison with multi-layer and slab models. *Boundary-Layer Meteorol*
540 101:329-358. DOI 10.1023/A:1019207923078
- 541 Kusaka, H., Kimura, F., 2004. Thermal effects of urban canyon structure on the nocturnal heat
542 island: Numerical experiment using a mesoscale model coupled with an urban canopy model.
543 *J Appl Meteorol* 43 (12), 1899–1910.
- 544 Liu Y, Chen F, Warner T, Basara J (2006) Verification of a mesoscale data-assimilation and
545 forecasting system for the Oklahoma City area during the Joint Urban 2003 field project. *J*
546 *Appl Meteorol Clim* 45:912-929.
- 547 Martilli A, Clappier A, Rotach MW (2002) An urban surface exchange parameterisation for
548 mesoscale models. *Boundary-Layer Meteorol* 104:261-304. DOI 10.1023/A:1016099921195
- 549 Martilli A (2007) Current research and future challenges in urban mesoscale modelling. *Int J*
550 *Climatol* 27:1909-1918. DOI 10.1002/joc.1620
- 551 Masson V (2000) A physically-based scheme for the urban energy budget in atmospheric models.
552 *Boundary-Layer Meteorol* 94:357-397. DOI 10.1023/A:1002463829265
- 553 Mauree D (2014) Development of a multi-scale meteorological system to improve urban climate
554 modeling. PhD thesis. Université de Strasbourg

- 555 Mauree, D., Kaempf, J. H., Scartezzini, J.-L., 2015. Multi-scale modelling to improve cli-
556 mate data for building energy models. In: Proceedings of the 14th International Confer-
557 ence of the International Building Performance Simulation Association. Hyderabad. <http://infoscience.epfl.ch/record/214837>
558
- 559 Mauree D, Blond N, Kohler M, Clappier A (2017) On the coherence in the boundary Layer:
560 Development of a Canopy Interface Model. *Front. Earth Sci.* 4:109. DOI 10.3389/feart.2016.
561 00109
- 562 Mauree, Dasaraden, Silvia Coccolo, Jrme Kaempf, et Jean-Louis Scartezzini. 2017. Multi-scale
563 modelling to evaluate building energy consumption at the neighbourhood scale. *PLOS ONE*
564 12 (9): e0183437. DOI <https://doi.org/10.1371/journal.pone.0183437>.
- 565 Mauree, Dasaraden, A. T. D. Perera, et Jean-Louis Scartezzini. 2017. Influence of Buildings
566 Configuration on the Energy Demand and Sizing of Energy Systems in an Urban Context.
567 *Energy Procedia*, 142 : 264854. DOI <https://doi.org/10.1016/j.egypro.2017.12.206>.
- 568 Mauree, Dasaraden, Daniel Sang-Hoon Lee, Emanuele Naboni, Silvia Coccolo, et Jean-Louis
569 Scartezzini. 2017. Localized meteorological variables influence at the early design stage. *Energy*
570 *Procedia*, 122 : 32530. DOI <https://doi.org/10.1016/j.egypro.2017.07.331>.
- 571 Monin AS, Obukhov AM (1954) Basic laws of turbulent mixing in the surface layer of the
572 atmosphere. *Contrib Geophys Inst Acad Sci USSR* 151:163-187.
- 573 Muller C (2007) Improvement of an urban turbulence parametrization for meteorological opera-
574 tional forecast and air quality modeling. PhD thesis. École Polytechnique Fédérale de Lausanne
- 575 National Centers for Environmental Prediction/National Weather Service/NOAA/U.S. Depart-
576 ment of Commerce. Updated daily. NCEP FNL Operational Model Global Tropospheric Anal-
577 yses, continuing from July 1999. Research Data Archive at the National Center for Atmospheric
578 Research, Computational and Information Systems Laboratory. Accessed 15 Sep 2017. DOI
579 <https://doi.org/10.5065/D6M043C6>
- 580 Oke TR (1982) The energetic basis of the urban heat island. *Q J R Meteorol Soc* 108:1-24.
581 DOI 10.1002/qj.49710845502
- 582 Omrani, H., Drobinski, P., Dubos, T., Mar. 2015. Using nudging to improve global-regional
583 dynamic consistency in limited-area climate modeling: What should we nudge? *Clim Dyn*
584 44 (5-6), 1627–1644.
585 URL <http://link.springer.com/article/10.1007/s00382-014-2453-5>
- 586 Ooyama KV (1990) A thermodynamic foundation for modeling the moist atmosphere. *J Atmos*
587 *Sci* 47:2580-2593.
- 588 Pohl, B., Crtat, J., Sep. 2014. On the use of nudging techniques for regional climate modeling:
589 application for tropical convection. *Clim Dyn* 43 (5-6), 1693–1714.
590 URL <http://link.springer.com/article/10.1007/s00382-013-1994-3>
- 591 Rotach, M. W., 1999. On the influence of the urban roughness sublayer on turbulence and
592 dispersion, *Atmos Environ* 33 (24): 4001-4008. DOI 10.1016/S1352-2310(99)00141-7
- 593 Rotach, M. W., R. Vogt, C. Bernhofer, E. Batchvarova, A. Christen, A. Clappier, B. Feddersen,
594 et al. 2005. BUBBLE an Urban Boundary Layer Meteorology Project. *Theor Appl Climatol*
595 81 (34): 23161. DOI <https://doi.org/10.1007/s00704-004-0117-9>.

Table A.4: Additional experiments run for theoretical case.

Simulations	Designation	Vertical resolution	Method
BEP-BEM+CIM	C2	Fine res. - 5m (15 levels)	FF
BEP-BEM+CIM	C4	Fine res. - 5m (15 levels)	FT

FF (fixed flux) and FT (fixed top) represent the two coupling methods.

596 Robinson, D., Nov. 2012. Computer modelling for sustainable urban design: Physical principles,
597 methods and applications. Routledge.

598 Salamanca F, Martilli A (2010) A new building energy model coupled with an urban canopy
599 parameterization for urban climate simulationspart II. Validation with one dimension off-line
600 simulations. Theor Appl Climatol 99:345-356. DOI 10.1007/s00704-009-0142-9

601 Salamanca F, Martilli A, Tewari M, Chen F (2011) A study of the urban boundary layer using
602 different urban parameterizations and high-resolution urban canopy parameters with WRF. J
603 Appl Meteorol Clim 50:1107-1128.

604 Sarkar A, De Ridder K (2011) The urban heat island intensity of paris: A case study based on
605 a simple urban surface parametrization. Boundary-Layer Meteorol 138:511-520. DOI 10.1007/
606 s10546-010-9568-y

607 Skamarock WC, Klemp JB, Dudhia J, et al (2008) A description of the advanced research WRF
608 version 2. DTIC Document

609 Skamarock WC, Klemp JB, Dudhia J, et al (2005) A description of the advanced research WRF
610 version 2. DTIC Document

611 **Appendix A. Supplementary Material**

612 *Appendix A.1. Additional experiments*

613 WRF is run for all the simulations using the BEP-BEM parameterization for the urban
614 effects. The vertical resolution, the use of CIM and the choice of the method are changed for the
615 different scenarios:

616 **Simulation C2** : WRF is run with the same resolution as the reference run with the CIM
617 coupled using Method FF. The BEP-BEM parametrization runs with the profiles calculated by
618 the CIM. This simulation is carried out to test whether the CIM has a significant effect when
619 WRF is running with a high resolution.

620 **Simulation C4** : WRF is run with a fine vertical resolution with the CIM coupled using Method
621 FT. This test is done to compare with the FF method.

622

623 *Appendix A.1.1. Comparison using a fine vertical grid resolution in the mesoscale model*

624 *Appendix A.1.2. Effect of the FF coupling with the CIM at high resolution - (Ref./C2)*

625 As expected the introduction the CIM in WRF with a high vertical resolution in the mesoscale
626 model (C2) did not have a significant impact on the simulation. Indeed its was shown that the
627 mesoscale simulations were not considerably modified when using a fine vertical grid resolution
628 in WRF. One can note from Table A.5 that the comparison with the high resolution simulation

Table A.5: Statistical comparison between the Reference Simulation (Ref.) and simulations C2 and C4.

Simulations	Method				
	FF	FT	Mean bias	R.M.S.E	R
<i>For Potential Temperature (K)</i>					
WRF+CIM+BEP-BEM					
Meso outputs at 50 m					
Fine Res. C2	x		0.0	0.1	1.00
Fine Res. C4		x	-0.1	0.3	1.00
<i>For Wind ($m s^{-1}$)</i>					
WRF+CIM+BEP-BEM					
Meso outputs at 50 m					
Fine Res. C2	x		0.2	0.3	1.00
Fine Res. C4		x	0.6	0.8	0.99

Comparisons are made for all the mesoscale outputs C2 and C4. FF (fixed flux) and FT (fixed top) represent the two coupling methods. Mean bias represents the deviation from the reference simulation, R.M.S.E is the root mean square error and R is the correlation. Meso outputs refers to outputs from the meso-scale model WRF at 50m which refers to the height at which the data is taken.

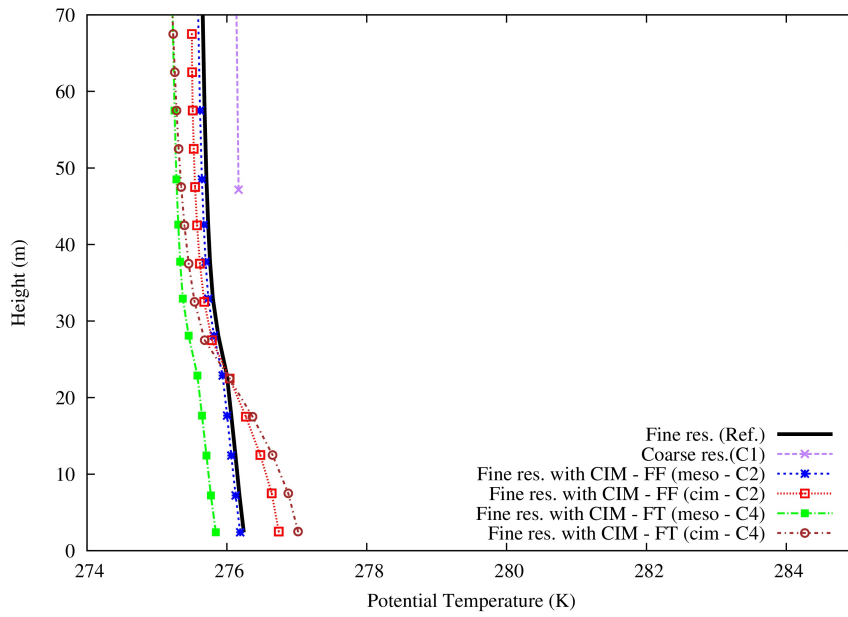
629 with the CIM gives satisfactory correlations. There were no difference on average for tempera-
630 ture and a small positive mean bias for the wind speed. It can hence be asserted that the CIM
631 is not bringing noteworthy changes in the WRF simulations when a very fine resolution is used
632 and hence that it is not deteriorating an already enhanced mesoscale simulation.

633
634 Similar to the comparison between the WRF fine resolution simulations and the WRF-CIM
635 simulations without taking into account the horizontal fluxes (C5), it can be noted here that for
636 C3 there is also an increase in the mean bias and the R.M.S.E for both the temperature and
637 the wind speed as compared to the reference simulation. The correlation coefficient for the wind
638 speed at 5 m is also drastically reduced.

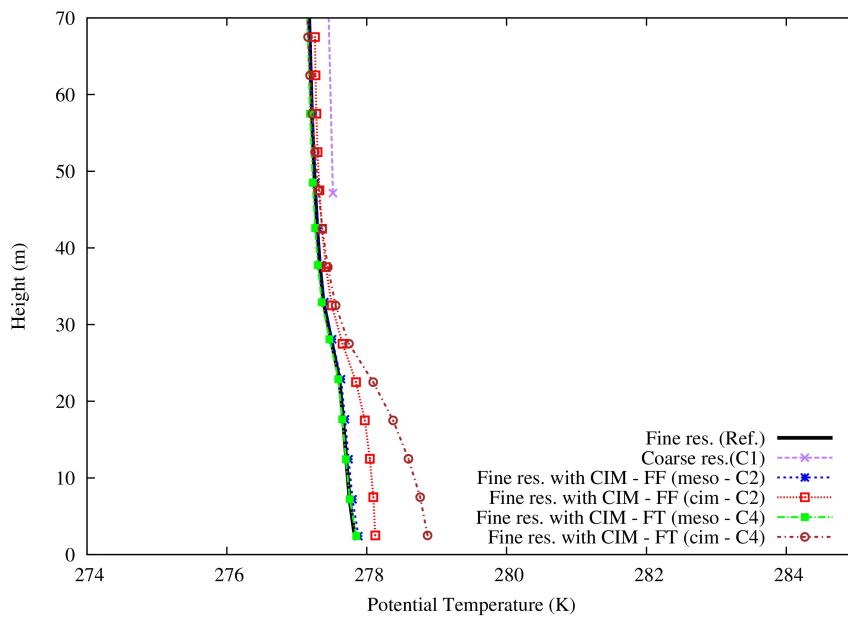
639 Figures [Appendix A.1](#) and [Appendix A.2](#) show the comparison between the vertical profiles
640 obtained by the mesoscale model when used at high resolution with or without the CIM (Ref.
641 and C2). We can note that the temperature profile from the mesoscale model is not modified
642 while the wind profile is slightly over-estimated in these cases. When the CIM is used, the effect
643 of the horizontal coupling is also tested by removing the horizontal fluxes in the CIM computa-
644 tion (C4). It turns out that the CIM with the horizontal fluxes gives profiles for the temperature
645 and wind that are close to the reference simulation, at both times in near-neutral or unstable
646 conditions. However, when these fluxes are not taken into account, there are changes in the
647 profiles both at the mesoscale level and in the CIM. The temperature is over-estimated (e.g., 1
648 K at 1700 LT in the CIM) close to the surface while the wind speed is further under-estimated
649 in the mesoscale model as compared to the solution with the FF method.

650
651 The effect of the correction can be noted on the profiles at 0200 LT with a disconnection at
652 the top of the column between CIM's profile and the mesoscale profile. This is due to the fact
653 that the correction forces CIM to give a mean value equal to the mesoscale mean value. This is
654 however not observed when the mixing is important (at 1700 LT).

655

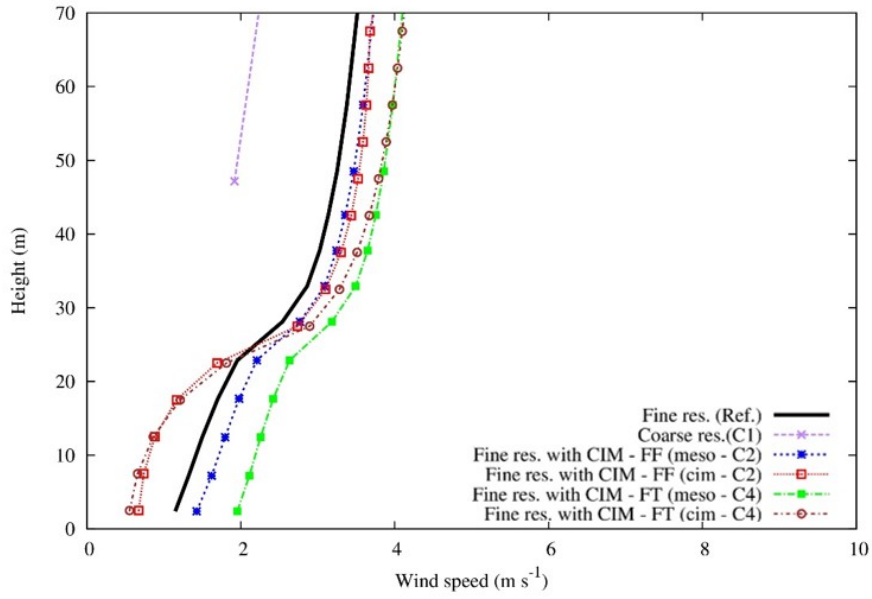


(a) At 0200 LT

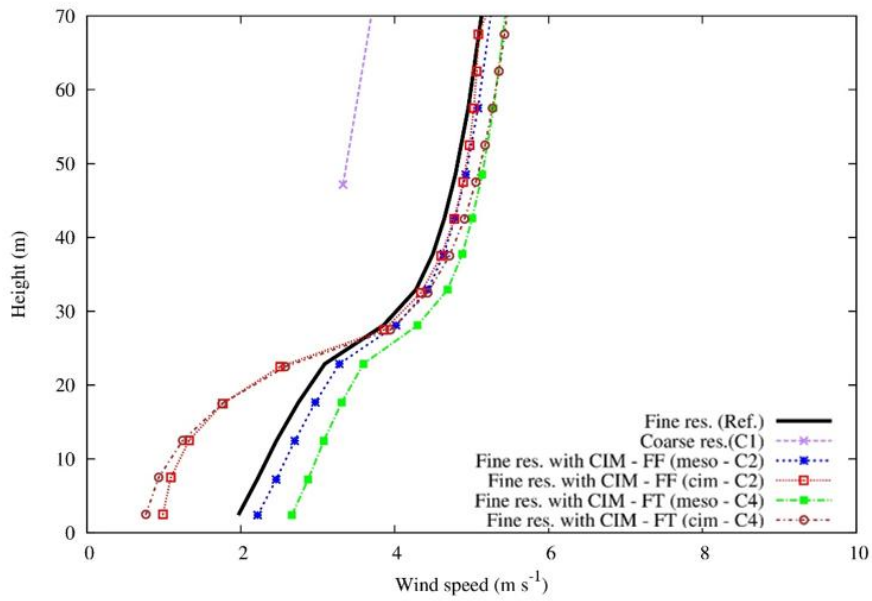


(b) At 1700 LT

Figure Appendix A.1: Profile of the potential temperature (in K) using a fine resolution (Ref. - bold black curve), coarse resolution (C1 - purple curve), fine resolution with the CIM (meso - C2 - blue curve ; cim - C2 - red curve) and fine resolution with the CIM - with no horizontal fluxes (meso - C4 - green curve ; cim - C4 - brown curve)



(a) At 0200 LT



(b) At 1700 LT

Figure Appendix A.2: Profile of the wind speed (in m s^{-1}) using a fine resolution with WRF (Ref. - bold black curve), coarse resolution (C1 - purple curve), fine resolution with the CIM (meso - C2 - blue curve ; cim - C2 - red curve) and fine resolution with the CIM - with no horizontal fluxes (meso - C4 - green curve ; cim - C4 - brown curve)